J Shoulder Elbow Surg (2022) 31, 1368–1375

ELSEVIER

Journal of Shoulder and Elbow Surgery

www.elsevier.com/locate/ymse

Analysis of the location and trajectory of the Kirschner wires in the fixation of extension-type supracondylar fracture of the humerus by 3D computational simulation

Wei Wang, MD[a], Qilin Li, MD[b], Allieu Kamara, MD, PhD[b], Zhitao Han, MD, PhD[c], Tianjing Liu, MD, PhD[b], Enbo Wang, MD, PhD[b,*]

[a]*Department of Trauma Orthopedics, Shengjing Hospital of China Medical University, Shenyang, Liaoning, China*
[b]*Department of Pediatric Orthopedics, Shengjing Hospital of China Medical University, Shenyang, Liaoning, China*
[c]*Department of Mathematics, College of Science, Northeastern University, Shenyang, Liaoning, China*

Background: Closed reduction and percutaneous pinning is still a preference for the treatment of supracondylar humerus fractures in children. However, no reports have shown the pin trajectory and the characteristics of the entry point so far. So we established a computational simulation model of the elbow to observe the trajectory of pinning for supracondylar humerus fractures.

Methods: We reconstructed an adult elbow computationally and simulated pin placement through lateral and medial pinning. Pin trajectories were traced after placement and after the addition of the skin profile; the relative entry points of the pins were determined. We used the center of the dorsal olecranon inflection as an anatomic reference for the entry points of lateral pinning. Four quadrants were established based on the center of the dorsal olecranon inflection: upper medial quadrant, upper lateral quadrant, lower medial quadrant, and lower lateral quadrant (LLQ).

Results: The maximum angle of pinning through the lateral column was 64° ± 3°. The minimum angles of pinning through the lateral column and middle column were 37° ± 3° and 20° ± 2°, respectively. The range of safe angle pinning through the medial column was between 18° ± 2° and 57° ± 3° to avoid penetration of the olecranon fossa and the cortex of the medial column. The entry points of lateral pinning were within the lateral half of the LLQ, and the lateral one-third of the LLQ contained all entry points of the pins through the lateral column and minor points of the pins through the middle column. The exit points of the medial pinning were within the lateral fringe of the metaphyseal-diaphyseal junction region; entering from the inferior two-thirds of the medial epicondyle could lead to the exit points in the proximal half of the metaphyseal-diaphyseal junction region laterally.

Discussion: For lateral pinning, the entry points would be within the lateral half of the LLQ. For the pins through the lateral column, the entry points should be within the lateral one-third of the LLQ. For medial pinning, entering from the inferior two-thirds of the medial epicondyle would lead to a more proximal exit.

Level of evidence: Basic Science Study; Computer Modeling

Keywords: Supracondylar humerus fractures; children; closed reduction and percutaneous pinning; computational simulation; trajectory; entry point; exit point

Approval for this study was received from the ethics institutional review board of Shengjing Hospital of China Medical University (2018PS361K).

*Reprint requests: Enbo Wang, MD, PhD, Department of Pediatric Orthopedics, The Shengjing Hospital of China Medical University, 36 Sanhao St, Heping District, Shenyang, Liaoning 110004, China.
E-mail address: wangenbodor@163.com (E. Wang).

https://doi.org/10.1016/j.jse.2021.12.048

Supracondylar humerus fractures (SHF) are the most common elbow injuries in children. It accounts for approximately 15% of all pediatric fractures.[2] Over 90% of SHF exhibit extension of the distal fragment.[17] SHF have been mainly classified into 3 main types according to the Gartland classification. The classic therapeutic management of Gartland extension type II and type III SHF is closed reduction and percutaneous pinning (CRPP).[3,6,14,17,18] Previous biomechanical studies have shown that both crossed pin and lateral pin fixation methods are stable configurations, which provide enough torsional rigidity.[11,19,22]

Although CRPP is currently the mainstream treatment of SHF, it still bears the risks of ulnar nerve injuries, postoperative elbow stiffness, and loss of reduction.[4,16] A report shows that nearly 18% of the patients who received CRPP experienced a loss of reduction.[6] One probable reason for this is intraoperative redirection attempts of the pins. Various angles and entry points are tried with personal experiences. Furthermore, multiple redirection attempts also increase the probability of neurovascular injuries. Even with intraoperative fluoroscopy, more considerations should be taken for the radiation of the C-arm for both patients and physicians.

To date, the optimal trajectories of pins used in CRPP have not been put forward. In our research, we reconstructed a 3-dimensional (3D) model of the distal humerus and simulated all possible favorable pin trajectories to determine the optimum range and zone of entry for a successful pin construct. We also superimposed the humerus model and simulated pin trajectories with the reconstructed skin in order to obtain surface markings for a deeper understanding of the pin trajectory, which may be of great help in the surgical techniques.

Materials and methods

Experimental materials

This is a 3D computational study of simulating the trajectories of the pins through the reconstructed elbow model. We had received the approval of our institutional review boards before we started the research. The data of the computed tomography (CT) scan of a volunteer (35-year-old man, healthy, African) were obtained with the right elbow in 2 different common positions as in the operation. The CT scan had a slice thickness of 1 mm (Ingenuity CT; Philips, Holland). The data of Digital Imaging and Communications in Medicine format were imported into Mimics Medical 17.0 (Materialise NV, Leuven, Belgium) for 3D reconstruction. Two 3D elbow models were constructed: (1) 140° flexion of the elbow (maximum active flexion) with the forearm in full pronation (140° model) and (2) 90° flexion of the elbow with the forearm in neutral position (90° model). Each model contained the cortical bone, cancellous bone, and skin profile.

Experimental procedure

The simulation of pin trajectories

The 2 mainstream configurations of pinning were simulated: crossed pinning and lateral pinning.[10,12,20] The entry points on the 140° model were simulated through the lateral condyle and medial epicondyle of the humerus model. The Kirschner wire was simulated as a rod with a diameter of 2 mm. The fracture line was assumed to be right on the interepicondylar line, as the typical fracture line of SHF in children.[1] We assumed the fixation to be stable when the entry and exit points were no less than 1 cm from the fracture line.[18] After the model pin was inserted, we checked it to make sure that the pin trajectory had no spatial overlaps of the bone cortex except the exit point. After the first check of trajectories, we tried to make the humeri of the 2 models (90° model and 140° model) completely overlap to exclude obstruction of the pin by the olecranon of the ulna and radial head in the 90° model (Fig. 1, *a*). For the 140° model, the center of the dorsal olecranon inflection (CDOI) was regarded as an anatomic reference. We established a plane (plane α in Fig. 1, *b*) through the dorsal olecranon inflection (CDOI), which was perpendicular to the coronal plane of the humerus. In the plane α, 2 perpendicular lines through the CDOI divided the plane into 4 quadrants, which were regarded as upper medial quadrant, upper lateral quadrant, lower medial quadrant, and lower lateral quadrant (LLQ) (Fig. 1, *c*).

According to the 3-column concept of Ji et al,[8] the lateral pinning would have to go through both the lateral column and the middle column (the olecranon fossa); we therefore simulated pinning trajectories of the lateral and middle columns.

Lateral entry simulation

In the previous research, Ji et al[8] found that in the 8 zones of the distal humerus, lateral pinning mainly exited between −2 zone and +1 zone (94.4%). Therefore, we selected 3 horizontal lines between +1 zone and −1 zone, between −1 zone and −2 zone, and between −2 zone and −3 zone. The intersections of these 3 parallel lines and the medial cortical border were regarded as the designated exit points, marked as point 0, point −1, and point −2 successively from proximal to distal (Fig. 2, *a*). In the middle column entry simulation, 4 designated points divided the medial edge of the olecranon fossa into 3 equal parts. In the coronal plane, the proximal 3 were selected as the passing-through points for the middle column pinning simulation (Fig. 2, *b*). Each pair of corresponding entry and passing-through points were marked with the same color.

As for the lateral view of the elbow, 4 parallel lines were drawn on the 140° model: (1) a line tangential to the dorsal aspect of the distal humerus (line *d*); (2) a line passed through the tip of the olecranon (line *c*); (3) a line passed through the CDOI (line *a*); and (4) a middle line between line *a* and line *c* (line *b*). These 4 lines divided the distal humerus into 3 zones, which were regarded as zone A, zone B, and zone C successively from anterior to posterior, respectively (Fig. 2, *c*). The angle between the pin and the paralleled lines was regarded as the pin entry angle in the sagittal plane. A pin that headed posterior to the humerus was regarded as a positive pin and that which headed anteriorly as a negative pin.

As for the lateral pinning in the coronal plane, we simulated the pin trajectory according to the following rules: (1) the medial

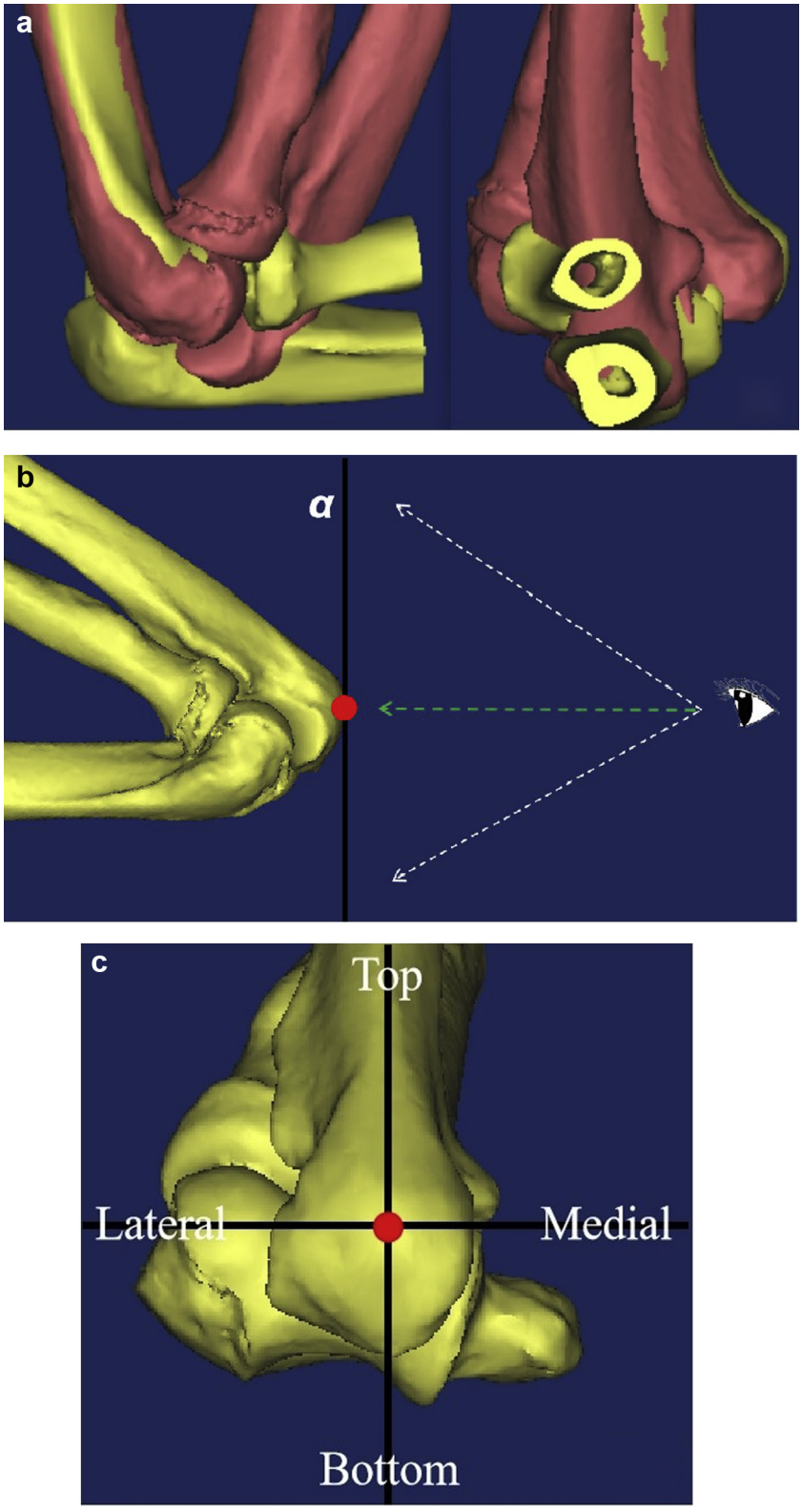

Figure 1 (**a**) Two models were simulated: 140° flexion of the elbow with the forearm in full pronation (*yellow*) and 90° flexion of the elbow with the forearm in neutral position (*brown*). These 2 models were overlapped to make sure that the olecranon and radial head do not obstruct the trajectory of the pin. (**b**) The plane α (*black*), which was perpendicular to the dorsal aspect of the distal humerus passed through the center of the dorsal olecranon inflection (CDOI) (*red point*). When the operator looks toward the CDOI, the plane α could be visualized, as shown in (**c**). (**c**) In the plane α, 2 perpendicular lines that passed through the CDOI were drawn and then 4 quadrants were obtained.

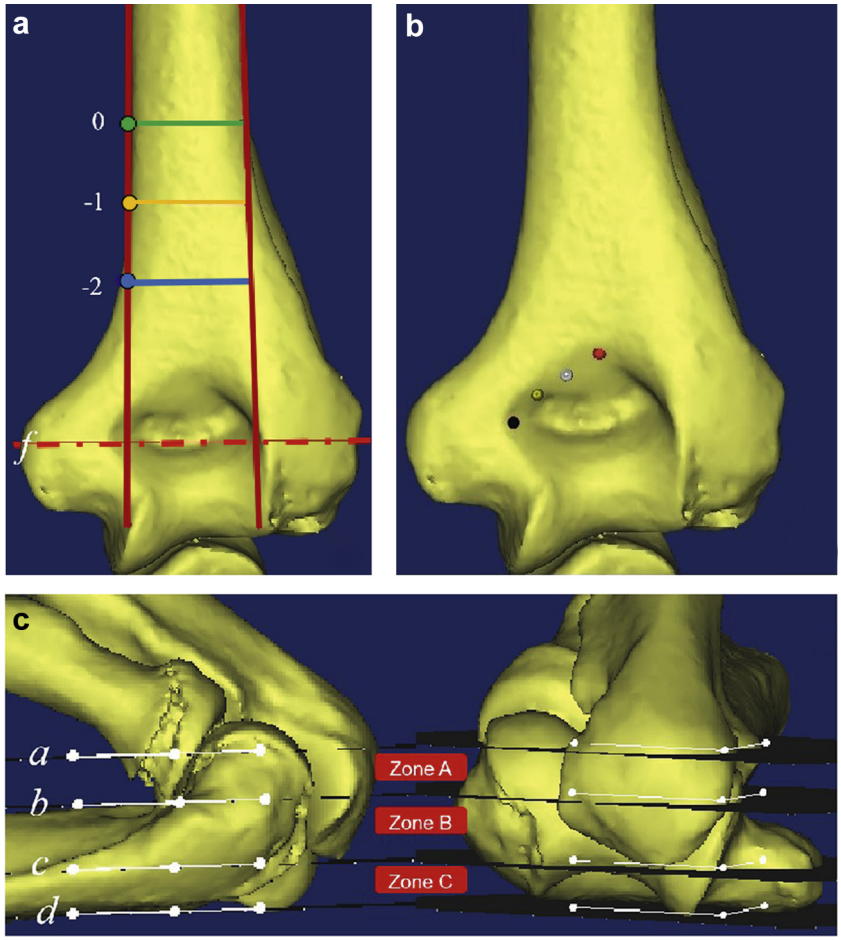

Figure 2 (**a**) A red horizontal line (line *f*) was regarded as the simulated fracture line (interepicondylar line) in the coronal plane. Three horizontal lines between +1 zone and −1 zone, −1 zone and −2 zone, and −2 zone and −3 zone were drawn (≡). These 3 parallel lines are running across the medial cortical fringe line at point 0, point −1, and point −2, respectively. (**b**) Three points (● ● ●) were selected as the designated passing-through points in the middle column pinning. (**c**) In the lateral view, 4 lines (lines *a*, *b*, *c*, and *d*) divided the lateral elbow into 3 zones: zone A, zone B, and zone C.

upper border of +1 zone was suggested as the designated exit point for the maximum angle simulation according to Ji et al,[8] and (2) all angles in the coronal plane were measured 3 times, and the medians were used in the end.

Medial entry simulation

We tried to find the most proximal and distal exit point in the lateral humeral cortex by simulating the medial pinning with various entry angles in the coronal plane, and the trajectories penetrating the olecranon fossa were excluded. While medial pinning, the exit points within the superior half were colored green and the points within the inferior half were colored red. Each pair of entry and exit points were drawn with the same color accordingly.

Combination with skin simulation

We reconstructed the elbow skin profile in Mimics and superimposed it with the humerus model and simulated pin trajectories in order to determine the relationship between the entry points and CDOI.

Results

Lateral entry simulation

The outline of the sets of the entry points pinning through the lateral column was found to be an irregular diamond shape (Fig. 3, *a*). Three different colors corresponded to the 3 designated exit points (point 0, point −1, and point −2). Similarly, the outline of the set of the entry points pinning through the middle column was found to be a diamond shape (Fig. 3, *b*).

In the sagittal plane, the entering angle from zone A ranged from 31° to 10°, from zone B from 21° to −6°, and from zone C from 7° to −5°.

In the coronal plane, the maximum angle of the pin through the lateral column was 64° ± 3°, whereas the minimum angles of the pin through the lateral column and through the middle column were 37° ± 3° and 20° ± 2°, respectively.

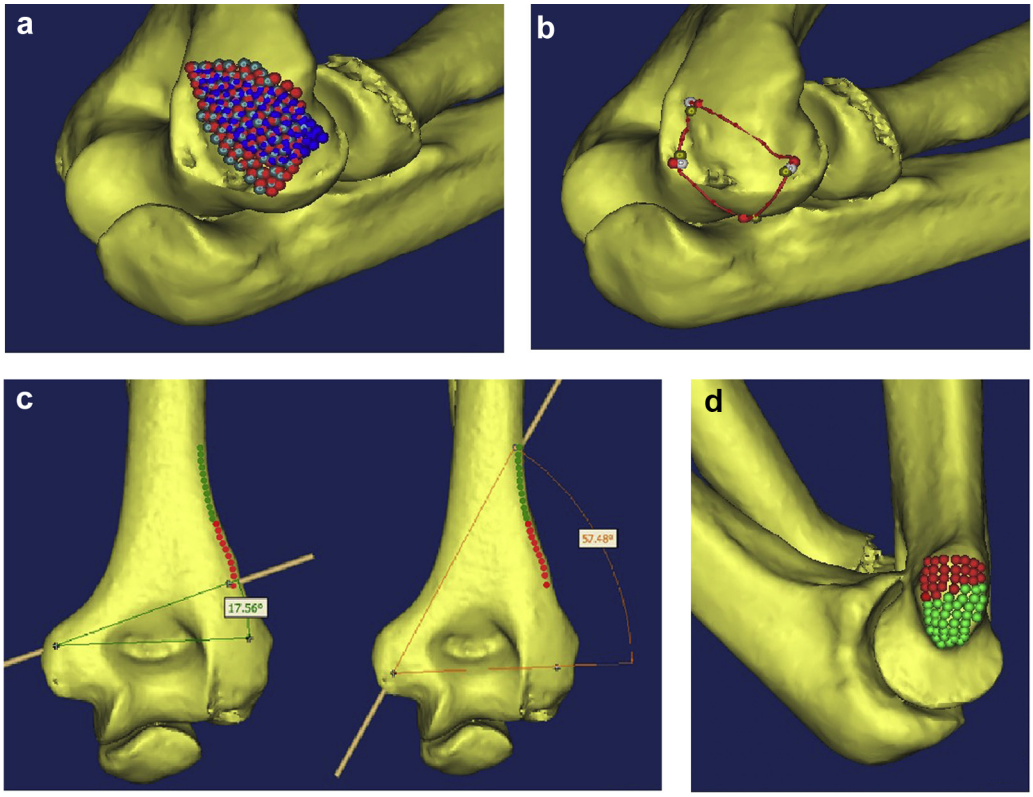

Figure 3 (**a**) The outline of the sets of lateral column entry points: the colors of the 3 sets corresponded with those of 3 designated exit points (point 0: ●, point -1: ●, and point -2: ●). (**b**) The outline of the set of the middle column entry points. (**c**) The ranges of angle in pinning from the medial epicondyle in the coronal plane; the exit points in the upper half of the metaphyseal-diaphyseal junction (MDJ) were colored *green* and in the lower half of the MDJ, *red*. (**d**) The sets of entry points in the medial epicondyle. The red points and the green points corresponded to the exit points in (**c**), respectively.

Medial entry simulation

The most proximal exit point was located in the distal humerus where it just became widened laterally (upper border of the metaphyseal-diaphyseal junction [MDJ]), and the most distal exit point was located slightly above the upper edge of the olecranon fossa (lower border of the MDJ). When entering from the medial epicondyle, the range of the angle in medial pinning was from $18° \pm 2°$ to $57° \pm 3°$ on the coronal plane (Fig. 3, *c*).The outline of the set of the entry points in the medial epicondyle was an inverted triangular shape (Fig. 3, *d*). Entering from the superior one-third of the medial epicondyle resulted in more distal exit points in the lower half of the MDJ region, whereas entering from the inferior two-thirds of the medial epicondyle resulted in more proximal exit points in the upper half of the MDJ region.

Combination with skin simulation

In the plane α, we measured the length of the 3 lines (line L, line L1, and line L2) in Figure 4, *b* and *c*, and calculated the ratio of L1/L and L2/L. The values were as follows: $L1/L = 0.51 \pm 0.01$ in Figure 4, *b*, 0.52 ± 0.01 in Figure 4, *c*, and $L2/L = 0.33 \pm 0.01$ in both Figure 4, *b* and *c*. So the set of the entry points of lateral pinning was within the lateral one-half of the LLQ, and the lateral one-third of the LLQ contained the entry points of the pins through the whole lateral column and a part of the middle column (Fig. 4, *a-c*).

Discussion

SHF is the most common fracture around the elbow joint in children.[3,6,13,17,18] The aim of treatment for SHF in children is to achieve good reduction and maintain that reduction through a stable percutaneous fixation, which could prevent re-displacement and deformity.[15] Currently, there are 2 common configurations of the percutaneous pinning technique: crossed pinning and lateral pinning.[5] The lateral pinning is preferred for the avoidance of nerve injury and the crossed pinning provides superior stability.[5,8,14] Currently, studies are more focused on the selection of configurations. However, there are few reports in the literature so far about the technique of pinning in practice, especially about how to locate the entry points and how to choose the angles explicitly while pinning. After successful

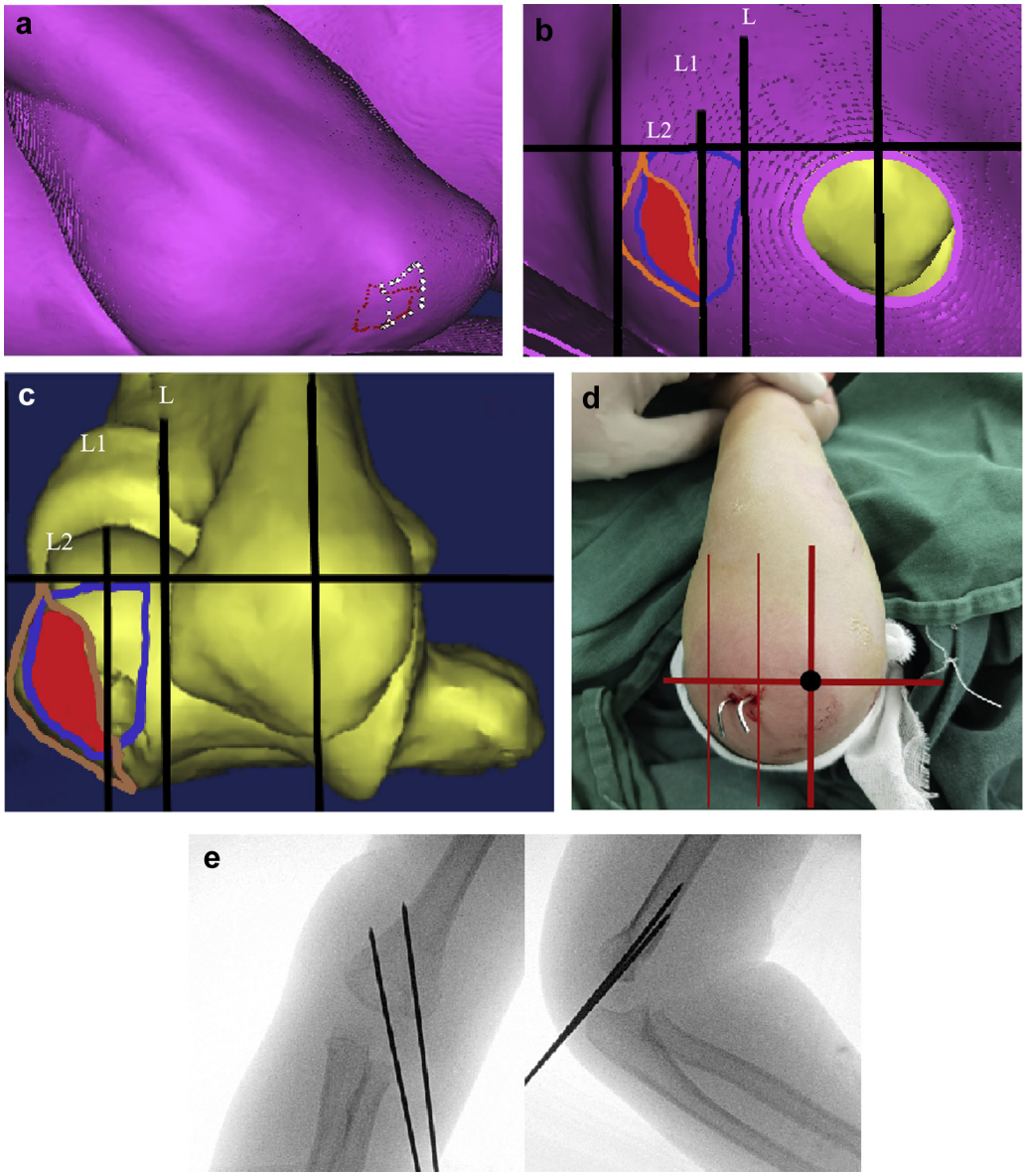

Figure 4 (**a**) The outline of the sets of entry points within the lateral condyle in the lateral view with combined skin reconstruction; the white outline was the set of entry points pinning through the middle column, and the red one was that of pinning through the lateral column. (**b**, **c**) In the plane α, the blue outline was the set of entry points pinning through the middle column, and the brown one was that of pinning through the lateral column. The red region was the overlapped area of entry points pinning through both lateral and middle column. (**d**) In the operation, the patient's elbow was held in maximum flexion with the forearm in full pronation after reduction. When the operator looks toward the CDOI (*black point*), the entry points of lateral pinning are within the lateral half of the lower lateral quadrant. (**e**) Anteroposterior and lateral intraoperative fluoroscopy of the elbow for the case in (**d**).

reduction, the choice of the entry point and the angle of pinning mainly depends on the surgeon's experience and the intraoperative fluoroscopic guidance. So there would be some failures, especially for the junior surgeon. Redirection is inevitable even with the guidance of fluoroscopy, which may lead to nearly 50% loss of pullout force by one time of redirection.[21] More attempts of redirection increase not only the risk of neurovascular injuries but also more exposure to radiation.[7] In our research, computational simulation was used on a 3D elbow model and the accurate trajectory of pinning was reproduced, and the location of entry points and the angle range of pinning would also be obtained. We also combined the bone reconstruction with the skin profile in order to find a reference in the pinning technique and increase the rate of successful pinning.

The CDOI is the most perceptible spot of the elbow intraoperatively after reduction, especially for the swollen elbow in the maximum passive flexion. The relative

position of the CDOI could be a solid anatomic reference for the entry point of lateral pinning.

For the entry points within the lateral condyle, we found that the outlines of the sets of the entry points pinning through the lateral column and the middle column were both irregular diamond shape. The set of entry points pinning through the middle column was slightly dorsal and medial to that of pinning through the lateral column, which indicated that the more dorsal and medial position should be chosen while middle column pinning.

In the lateral view, zone A and zone B were level with the upper and lower half respectively of the olecranon arc, which would serve as a good intraoperative reference. The angle ranges of the 3 zones (zone A, zone B, and zone C) were different. According to the angle ranges obtained, we found that the trajectory should head a little bit posteriorly to the dorsal aspect of the humerus while entering from zone A, parallel or slightly posteriorly while entering from zone B, and slightly anteriorly while entering from zone C. Therefore, in practice, intraoperatively, if the surgeon prefers the crossing pin configuration on sagittal plane, 1 pin pointed posteriorly (positive pin) would enter in zone A or zone B and the other pin pointed anteriorly (negative pin) would enter in zone B or zone C, accordingly.

In the coronal plane of the humerus, the maximum angle of the lateral pinning was 64° ± 3°. In the operation, pinning through the lateral column is intentionally aimed as proximal as we can to obtain the more divergent configuration. According to Ji et al,[8] only 5.6% of the exit points were superior to the upper border of +1 zone. So we regarded the medial upper border of +1 zone as the most superior exit point in practice. Intraoperatively, we should beware that if the angle of the lateral condyle trajectory is beyond this maximum angle of our simulation, the pin is likely to slip into the medullary canal. The minimum angles of simulated pinning through the lateral column and the middle column were 37° ± 3° and 20° ± 2°, respectively, which indicated that while pinning laterally, the trajectory angle should be more or less greater than the minimum angle of simulation to improve the success rate.

For entry from the medial epicondyle, we found that the range of the exit points of the medial pinning was within the lateral fringe of the MDJ region. It is suggested that entering from the inferior two-thirds of the medial epicondyle of the humerus could lead to the more proximal exit point. However, the entry point through the medial epicondyle is not usually that low due to the irritation of the ulnar nerve by the wires probably.[9] Commonly, less than 90° flexion of the elbow is generally preferred while pinning from the medial epicondyle, and the entry point from the medial epicondyle is often above the bottom of the medial epicondyle.[5]

We found that if the angles were less than 18° ± 2° for the medial pinning on the coronal plane, the pins may penetrate the olecranon fossa even though the pin entering from the superior of the medial epicondyle. We would also find it difficult to achieve a greater angle more than 57° ± 3° for the medial pinning on the coronal plane because of the blockage of the cortex of medial column and the risk of irritation to the ulnar nerve.

Combined with the simulation of skin reconstruction in the plane α, it was found that the entry points of the lateral pinning were totally within the lateral one-half of the LLQ. It is shown that the proper region for lateral pinning is within the scope of the lateral half of the LLQ. The lateral one-third of the LLQ contained the entry points of the whole lateral column pinning and partial middle column pinning. Therefore, the entry points would be within the lateral one-third of the LLQ while performing the lateral column pinning.

The preferred pinning of CRPP treatment is usually through the lateral column first.[9] We followed this method and managed according to the current research for the first pinning; we keep the elbow in maximum passive flexion (approximately 140°) with the forearm in full pronation after reduction, and the CDOI could be regarded as a reference. When the operator looks toward the elbow, the entry point of the first pin is within the lateral one-third of the LLQ and levels with the arc of olecranon (zones A and B); then we drill the pin with a proper angle according to the results mentioned above. After the first pinning, the second pinning would be through the middle or medial column as the operator's preference under the rules suggested above (Fig. 4, *d* and *e*). These techniques would significantly decrease the amount of radiation exposure intraoperatively.

As far as we know, this is the first pinning trajectory research by computational simulation of supracondylar fracture in children, which contains some limitations: first, the research is only based on the computational simulation. The results would be more convincing with cadaver research. Secondly, this study is based on the elbow simulation of an adult, which could not sufficiently reflect the circumstance of a pediatric patient. Pediatric CT scans cannot depict the morphology of the cartilage, so that we cannot reconstruct a normal elbow with pediatric data. Thirdly, the research did not include all types of SHF in children, such as flexion-type fracture, which requires different techniques in closed reduction and pinning.

Conclusions

The CDOI could be regarded as an anatomic reference for entry point selection in lateral pinning for well-reduced extension-type SHF in children. The entry points of the lateral pinning should be within the lateral half of the lower lateral quadrant, and the entry points of the pins through the lateral column should be within the lateral one-third of the lower lateral quadrant. The range of the angles between 18° ± 2° and 57° ± 3° on the

coronal plane would be relatively safe while medial pinning. The exit points of the medial pinning would be within the lateral fringe of the MDJ region, and entering from the inferior two-thirds of the medial epicondyle would lead to the more proximal exit point.

Disclaimers:

Funding: This work was supported by the 345 Talent Project of Shengjing Hospital (M0279, M0746), the Youth Talent Cultivation Program of China Medical University(Tianjing Liu), Liaoning Science and Technology Major Projects (M0806-19, M0806-22).
Conflicts of interest: The authors, their immediate families, and any research foundations with which they are affiliated have not received any financial payments or other benefits from any commercial entity related to the subject of this article.

References

1. Bahk MS, Srikumaran U, Ain MC, Erkula G, Leet AI, Sargent MC, et al. Patterns of pediatric supracondylar humerus fractures. J Pediatr Orthop 2008;28:493-9. https://doi.org/10.1097/BPO.0b013e31817bb860
2. Barr LV. Paediatric supracondylar humeral fractures: epidemiology, mechanisms and incidence during school holidays. J Child Orthop 2014;8:167-70. https://doi.org/10.1007/s11832-014-0577-0
3. Bloom T, Robertson C, Mahar AT, Newton P. Biomechanical analysis of supracondylar humerus fracture pinning for slightly malreduced fractures. J Pediatr Orthop 2008;28:766-72. https://doi.org/10.1097/BPO.0b013e318186bdcd
4. Bogdan A, Quintin J, Schuind F. Treatment of displaced supracondylar humeral fractures in children by humero-ulnar external fixation. Int Orthop 2016;40:2409-15. https://doi.org/10.1007/s00264-016-3251-y
5. Carrazzone OL, Barbachan Mansur NS, Matsunaga FT, Matsumoto MH, Faloppa F, Belloti JC, et al. Crossed versus lateral K-wire fixation of supracondylar fractures of the humerus in children: a meta-analysis of randomized controlled trials. J Shoulder Elbow Surg 2021;30:439-48. https://doi.org/10.1016/j.jse.2020.09.021
6. Holland P, Highcock A, Bruce C. Distance of translation as a predictor of failure of fixation in paediatric supracondylar fractures. Ann R Coll Surg Engl 2017;99:524-8. https://doi.org/10.1308/rcsann.2017.0040
7. Hsu RY, Lareau CR, Kim JS, Koruprolu S, Born CT, Schiller JR. The effect of C-arm position on radiation exposure during fixation of pediatric supracondylar fractures of the humerus. J Bone Joint Surg Am 2014;96:e129. https://doi.org/10.2106/JBJS.M.01076
8. Ji X, Kamara A, Wang E, Liu T, Shi L, Li L. A two-stage retrospective analysis to determine the effect of entry point on higher exit of proximal pins in lateral pinning of supracondylar humerus fracture in children. J Orthop Surg Res 2019;14:351. https://doi.org/10.1186/s13018-019-1400-x
9. Kocher MS, Kasser JR, Waters PM, Bae D, Snyder BD, Hresko MT, et al. Lateral entry compared with medial and lateral entry pin fixation for completely displaced supracondylar humeral fractures in children. A randomized clinical trial. J Bone Joint Surg Am 2007;89:706-12. https://doi.org/10.2106/JBJS.F.00379
10. Ladenhauf HN, Schaffert M, Bauer J. The displaced supracondylar humerus fracture: indications for surgery and surgical options: a 2014 update. Curr Opin Pediatr 2014;26:64-9. https://doi.org/10.1097/MOP.0000000000000044
11. Larson L, Firoozbakhsh K, Passarelli R, Bosch P. Biomechanical analysis of pinning techniques for pediatric supracondylar humerus fractures. J Pediatr Orthop 2006;26:573-8. https://doi.org/10.1097/01.bpo.0000230336.26652.1c
12. Lee YH, Lee SK, Kim BS, Chung MS, Baek GH, Gong HS, et al. Three lateral divergent or parallel pin fixations for the treatment of displaced supracondylar humerus fractures in children. J Pediatr Orthop 2008;28:417-22. https://doi.org/10.1097/BPO.0b013e318173e13d
13. Liebs TR, Burgard M, Kaiser N, Slongo T, Berger S, Ryser B, et al. Health-related quality of life after paediatric supracondylar humeral fractures. Bone Joint J 2020;102-B:755-65. https://doi.org/10.1302/0301-620X.102B6.BJJ-2019-1391.R2
14. Liu C, Kamara A, Liu T, Yan Y, Wang E. Mechanical stability study of three techniques used in the fixation of transverse and oblique metaphyseal-diaphyseal junction fractures of the distal humerus in children: a finite element analysis. J Orthop Surg Res 2020;15:34. https://doi.org/10.1186/s13018-020-1564-4
15. Mulpuri K, Tritt BL. Low incidence of ulnar nerve injury with crossed pin placement for pediatric supracondylar humerus fractures using a mini-open technique. J Orthop Trauma 2006;20:234. https://doi.org/10.1097/00005131-200603000-00014
16. Sankar WN, Hebela NM, Skaggs DL, Flynn JM. Loss of pin fixation in displaced supracondylar humeral fractures in children: causes and prevention. J Bone Joint Surg Am 2007;89:713-7. https://doi.org/10.2106/JBJS.F.00076
17. Shore BJ, Gillespie BT, Miller PE, Bae DS, Waters PM. Recovery of motor nerve injuries associated with displaced, extension-type pediatric supracondylar humerus fractures. J Pediatr Orthop 2019;39:e652-6. https://doi.org/10.1097/BPO.0000000000001056
18. Skaggs DL, Cluck MW, Mostofi A, Flynn JM, Kay RM. Lateral-entry pin fixation in the management of supracondylar fractures in children. J Bone Joint Surg Am 2004;86:702-7. https://doi.org/10.2106/00004623-200404000-00006
19. Skaggs DL, Hale JM, Bassett J, Kaminsky C, Kay RM, Tolo VT. Operative treatment of supracondylar fractures of the humerus in children. The consequences of pin placement. J Bone Joint Surg Am 2001;83:735-40.
20. Srikumaran U, Tan EW, Belkoff SM, Marsland D, Ain MC, Leet AI, et al. Enhanced biomechanical stiffness with large pins in the operative treatment of pediatric supracondylar humerus fractures. J Pediatr Orthop 2012;32:201-5. https://doi.org/10.1097/BPO.0b013e31824536c8
21. Vercio RC, Anderson M, Thomas A, Inceoglu S, Wongworawat MD. K-wire pull-out force after multiple redirection attempts. J Hand Surg Am 2018;43:1081-4. https://doi.org/10.1016/j.jhsa.2018.09.005
22. Zionts LE, McKellop HA, Hathaway R. Torsional strength of pin configurations used to fix supracondylar fractures of the humerus in children. J Bone Joint Surg Am 1994;76:253-6.